SIEMENS

Reprint

Parallel Transmission and its Clinical Implementation: Enabling new Clinical Imaging Paradigms

Fernando Boada; Tim Shepherd; Andrew Rosenkrantz; Eric E. Sigmund; Jurgen Fütterer; Hersh Chandarana; Mari Hagiwara; Henry Rusinek; Artem Mikheev; Mary Bruno; Christian Geppert; Christopher Glielmi; Josef Pfeuffer

Reprint from the customer magazine MAGNETOM Flash, February 2013, Pages 4–10

Answers for life.

Parallel Transmission and its Clinical Implementation: Enabling new Clinical Imaging Paradigms

Fernando Boada[1]; Tim Shepherd[1]; Andrew Rosenkrantz[1]; Eric E. Sigmund[1]; Jurgen Fütterer[2]; Hersh Chandarana[1]; Mari Hagiwara[1]; Henry Rusinek[1]; Artem Mikheev[1]; Mary Bruno[1]; Christian Geppert[3]; Christopher Glielmi[3]; Josef Pfeuffer[3]

[1]*Department of Radiology NYU Langone Medical Center, New York, NY, USA*
[2]*Department of Radiology, Radboud University Nijmegen Medical Centre, Nijmegen, The Netherlands*
[3]*Siemens Healthcare*

Introduction

The use of multiple and independent receive channels to accelerate MR data acquisition has enabled numerous clinical applications that are now part of the standard clinical workflow at state-of-the-art imaging centers. Parallel transmission (pTX) was, likewise, introduced as a means to enable and improve the use of extended RF excitations schemes such as multidimensional spatially-selective excitation, which, although conceptually powerful, were previously rendered impractical due to their long RF pulse durations.

The 3T MAGNETOM Skyra is the first clinical system to feature a parallel transmission architecture capable of enabling applications beyond B_1 shimming. This revolutionary capability allows enhancing the performance and reliability of several imaging sequences that are essential for advanced clinical applications. These enhancements are particularly significant at 3T, where B_1 field inhomogeneity can be problematic over large fields-of-view (FOV). We present several examples where the role of this technology demonstrates clinical benefits by enabling previously impractical imaging paradigms and/or improving the performance of existing ones.

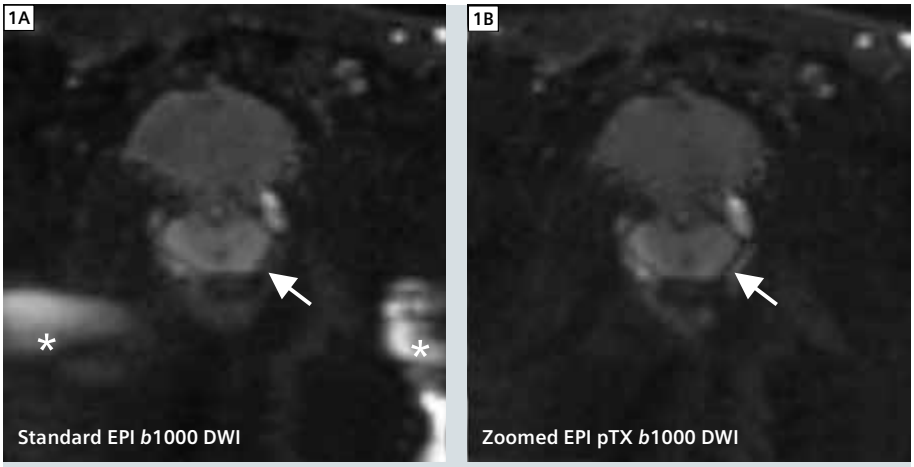

1 Standard *b*1000 image **(1A)** shows wrap artifact (*) not present on zoomed EPI image **(1B)**. There is greater clarity of prostate capsule on zoomed EPI (arrow, 1A and 1B).

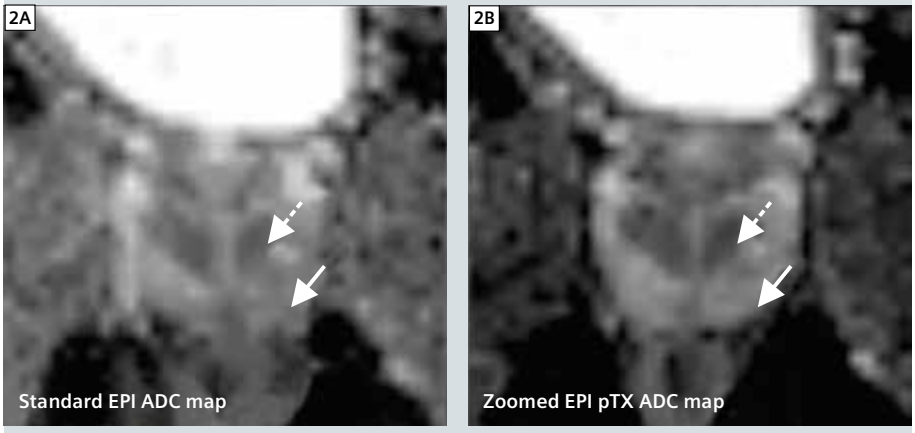

2 There is greater clarity of prostate capsule (solid arrow) and of transition zone boundary (dotted arrow) on zoomed EPI image **(2B)** than on standard EPI **(2A)**.

Table 1: Comparison of standard and zoomed DWI.

Feature	Standard EPI	Zoomed EPI
b1000 s/mm² images		
Absence of ghosting artifact	3.8 ± 0.4	4.3 ± 0.5
Absence of wrap artifact	3.7 ± 0.8	4.7 ± 0.5
Clarity of prostate capsule	4.0 ± 0.0	4.8 ± 0.4
Clarity of peri-urethral region	3.5 ± 0.5	4.2 ± 1.0
Overall image quality	3.7 ± 0.5	4.0 ± 0.6
ADC maps		
Reduced distortion of prostate	3.5 ± 0.5	3.8 ± 0.4
Clarity of transition zone boundary	3.2 ± 0.8	3.5 ± 0.4
Clarity of prostate capsule	3.2 ± 9.4	3.8 ± 0.4
Overall image quality	3.2 ± 0.4	3.7 ± 0.5
ADC (x 10^{-3} mm^2/s)	1.34 ± 0.3	1.41 ± 0.8

Skyra pTX architecture

The Skyra pTX system builds upon the existing clinical MAGNETOM Skyra platform, namely, a 3T magnet with a 70 cm patient bore diameter and parallel RF excitation via two fully independent, phase-coherent RF channels (TimTX TrueShape). The two pTX RF channels allow extended dynamic RF excitation schemes using a two-channel RF body coil. State-of-the-art imaging gradients (45 mT/m peak amplitude, 200 mT/m/s slew rate) and a full complement of Tim 4G multi-channel receive coils round out the hardware configuration of the system. The scanner operates under software version *syngo* MR D13C providing full access to further new technologies such as Dot, *syngo* REVEAL etc. While there are pTX features that can be applied during the adjustments (patient-specific B_1-shimming, volume-selective B_1-shimming), we have focused on the improved sequences and applications which provide new features with pTX. This includes 2D-selective RF pulses with an echo-planar TX trajectory that excite a selective volume (so-called 'inner-volume') and allows to reduce the FOV in the phase direction [1, 2] for zoomed echo planar imaging (EPI) (*syngo* ZOOMit).

§ Firevoxel and Igor Pro are not Siemens Healthcare products. Siemens bears no responsibility for these products including, but not limited to, their regulatory status.

Prostate imaging

Diffusion-weighted imaging (DWI) is a critical sequence for prostate cancer detection and localization, but often suffers from spatial-distortion EPI artifacts related to the field inhomogeneity induced by the neighboring air spaces; these challenges can be more problematic at 3T. In this challenging imaging scenario, 2D-selective zoomed EPI in conjunction with a more homogeneous localized (B_1-shimmed) RF excitation can be particularly helpful. The impact of zoomed EPI on image quality of prostate DWI at 3T was assessed in six volunteers who underwent prostate MRI using an 18-channel body matrix receive coil. Scans included a single-shot EPI DWI sequence (*b*-values 50, 500, and 1000 s/mm²) performed with a regular sinc pulse ('Standard') and with the advanced 2D spatially selective RF pulse ('ZOOMit') combined with a reduced FOV approach (zoomed EPI). The *b*1000 images and ADC maps were assessed for various image quality measures on a scale from 1 to 5 (5 = highest image quality). Also, peripheral zone (PZ) ADC and estimated signal-to-noise (eSNR: determined as mean/SD of PZ) on *b*1000 images were measured. These measures were compared between standard and zoomed EPI.

Compared with standard EPI, zoomed EPI *b*1000 images showed improvements in ghosting, wraparound artifacts, clarity of prostate capsule, and clarity of peri-urethral region (Fig. 1, Table 1). By contrast, zoomed EPI ADC maps showed improvements in clarity of prostate capsule and overall image quality (Fig. 2). eSNR was nearly identical between standard and zoomed EPI *b*1000 images. The prostate showed a small increase in mean ADC on zoomed EPI images (mean increase 0.07 x 10^{-3} mm^2/s). However, ADC reproducibility between standard and zoomed EPI DWI remained high (mean coefficient of variability of ADC (4.4 ± 4.0)%, range 0.3 to 11.0%).

This preliminary assessment showed improvements in numerous measures relating to artifacts and anatomic clarity

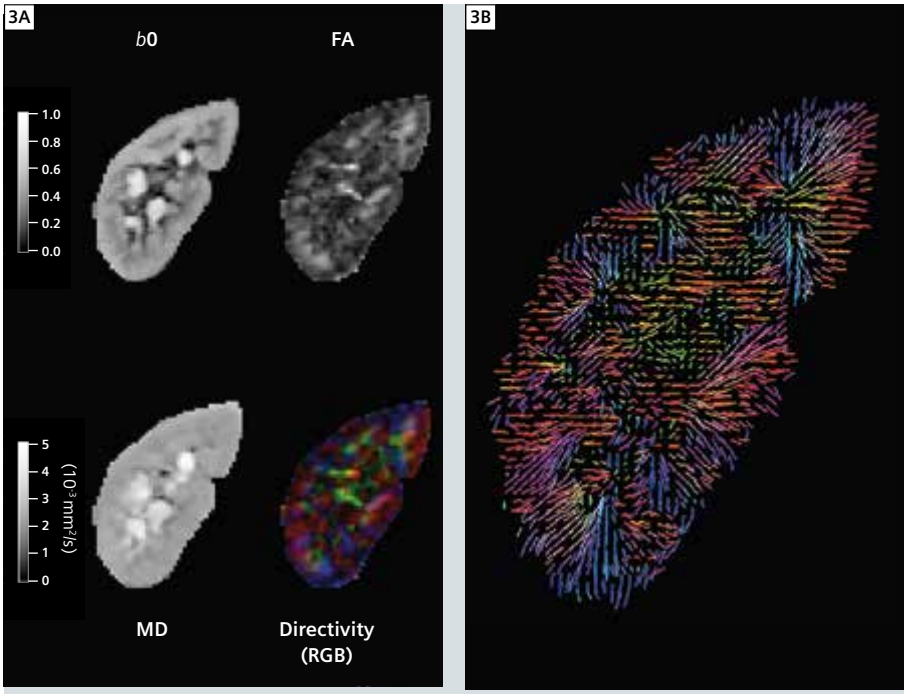

3 Kidney Zoomed-EPI DTI images.
(3A) Images obtained with *b*0 sec/mm², fractional anisotropy (FA) map, mean diffusivity (MD) map, and direction-encoded color map. Medullary anisotropy is evident in the FA map.
(3B) Color-coded primary diffusion eigenvectors display radial pattern of medullary tubules.

when applying 2D-selective zoomed EPI with for prostate DWI at 3T. While the FOV was held fixed to ensure comparability between the sequences, the use of a smaller FOV is easily achieved with zoomed EPI and currently under investigation. Nonetheless, even without this adjustment, zoomed DW-EPI using 2-channel pTX has potential to improve image quality for DWI of the prostate at 3T.

Renal imaging

Diffusion-tensor imaging (DTI) uses multiple diffusion sensitizing directions to evaluate anisotropic microstructure and is a promising imaging technique for the functional assessment of kidneys. Microstructure is a key factor in renal physiology, where cortex contains randomly oriented structures, while medulla holds more aligned vessel and tubular networks. Kidney DTI has shown that renal medulla has inherently higher fractional anisotropy (FA) in comparison with the isotropic cortex [2-4]. However, kidney DTI using single-shot spin-echo EPI typically suffers from imaging artifacts such as field-inhomogeneity-related distortions, and low spatial resolution due to the matrix size and long echo trains required for abdominal imaging. In this context, shortening the echo train length could reduce the aforementioned distortions. To achieve the same level of spatial resolution, while keeping a shorter echo train length, the imaging FOV must be reduced along the phase direction by the same factor used to shorten the echo train length. Zoomed EPI achieves such a goal through the use of 2D-selective RF excitation.
Four consecutive healthy volunteers without any history of renal disease (three males, one female; mean age 28 (24-30 years); non-fasting conditions) were imaged on the Skyra pTX system. Free-breathing single-shot 2D-selective zoomed EPI DW images were acquired with reduced FOV in the left-right direction with the following parameters: 10-14 coronal slices, slice thickness 4 mm, no gap; FOV of 83 x 400 mm; 64 x 308 acquisition matrix, 1.3 mm resolution, TR 4000 ms; TE 65 ms; six diffusion directions; monopolar diffusion gradients; two *b*-values (*b*0 and *b*500 s/mm²); parallel imaging (GRAPPA) factor of two and scan time 5:28 min. An additional saturation band was applied to suppress signal from the left side of the body extending slightly beyond the stop-band. Right kidney images were co-registered by using a two-dimensional rigid body transform algorithm, and MR images at the same *b*-value and direction were then averaged by using locally developed software (Firevoxel[§]). DT processing was performed with custom software written in Igor Pro[§] (Wavemetrics, Portland, OR, USA). Parametric maps were generated of DTI eigenvalues λ_i and eigenvectors, mean diffusivity (MD) and fractional anisotropy (FA). The ZOOMit DTI technique allowed for high quality diffusion images of the kidney with reduced blurring and distortion (Fig. 3) compared to full FOV EPI DTI. Medullary anisotropy and radial orientation pattern was evident in all volunteers (e.g. Fig. 3). The medullary / cortical MD and FA values were 2.04 ± 0.14 / 2.21 ± 0.12 μm²/ms, and 0.34 ± 0.08 / 0.13 ± 0.04, respectively, consistent with literature [3-5]. MD showed significantly higher, and FA significantly lower, cortical than medullary values. ZOOMit DTI may be valuable for clinical assessment of kidney pathology, particularly for applications closely scrutinizing corticomedullary differentiation.

Breast imaging

Diffusion-weighted imaging (DWI) of the breast is increasingly used for the differential diagnosis and treatment response monitoring of breast cancer. Conventional EPI techniques are prone to characteristic artifacts, such as susceptibility artifacts, image blurring and spatial distortion resulting from gradient nonlinearity and eddy currents. Thus, there can be a significant mismatch in lesion appearance and position between morphologic sequences and EPI which

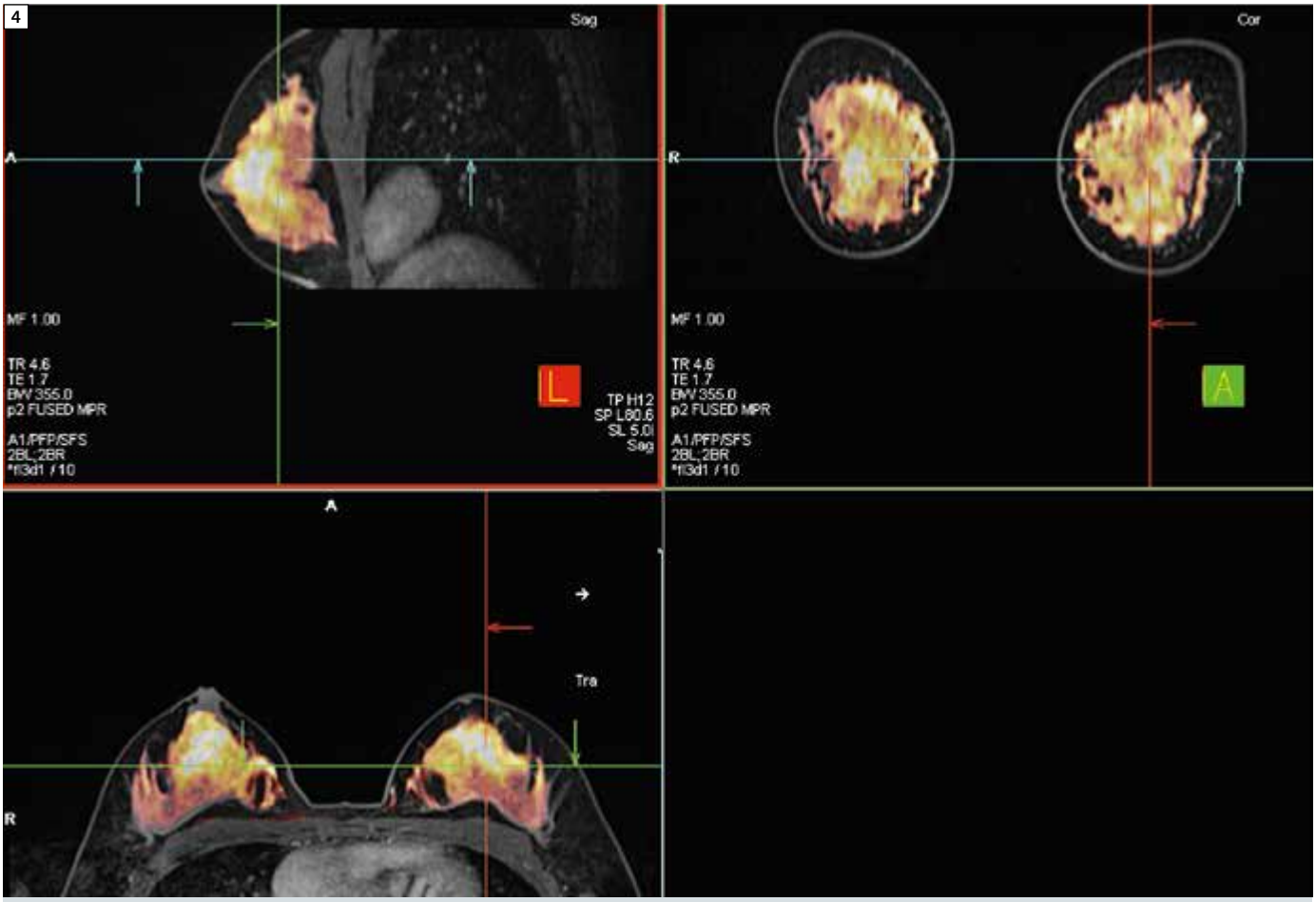

4 T1-weighted VIBE fused with a diffusion-weighted (*b*400) dataset.

can potentially affect the diagnostic accuracy. In addition, the strong demand on the gradient system limits the spatial resolution to only moderate in-plane resolution around 1.8 x 1.8 mm^2 or even coarser. Thus spatially-selective excitation with EPI ZOOMit was applied to a) mitigate the spatial distortion by shortening the phase encode burden and the echo train length and b) to allow the user to restrict the acquisition volume to the breast alone resulting in a higher spatial resolution.

3 healthy subjects were scanned using a 4-channel combined (biopsy and diagnostic) breast coil. For comparison, in both protocols 24 axial slices were acquired with three b-values in 3-scan trace mode with GRAPPA factor of 2. The nominal in-plane resolution was 1.8 x

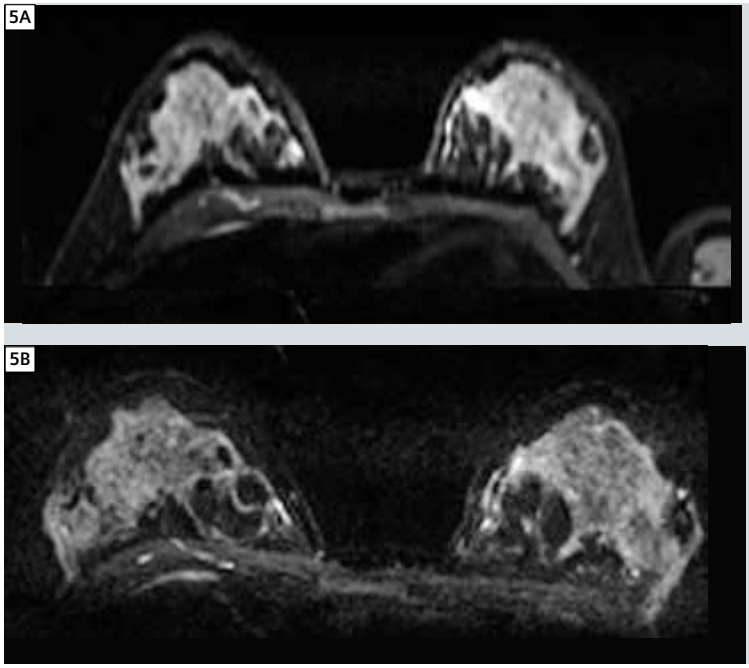

5 Standard DW-EPI **(5A)** and zoomed EPI **(5B)**.

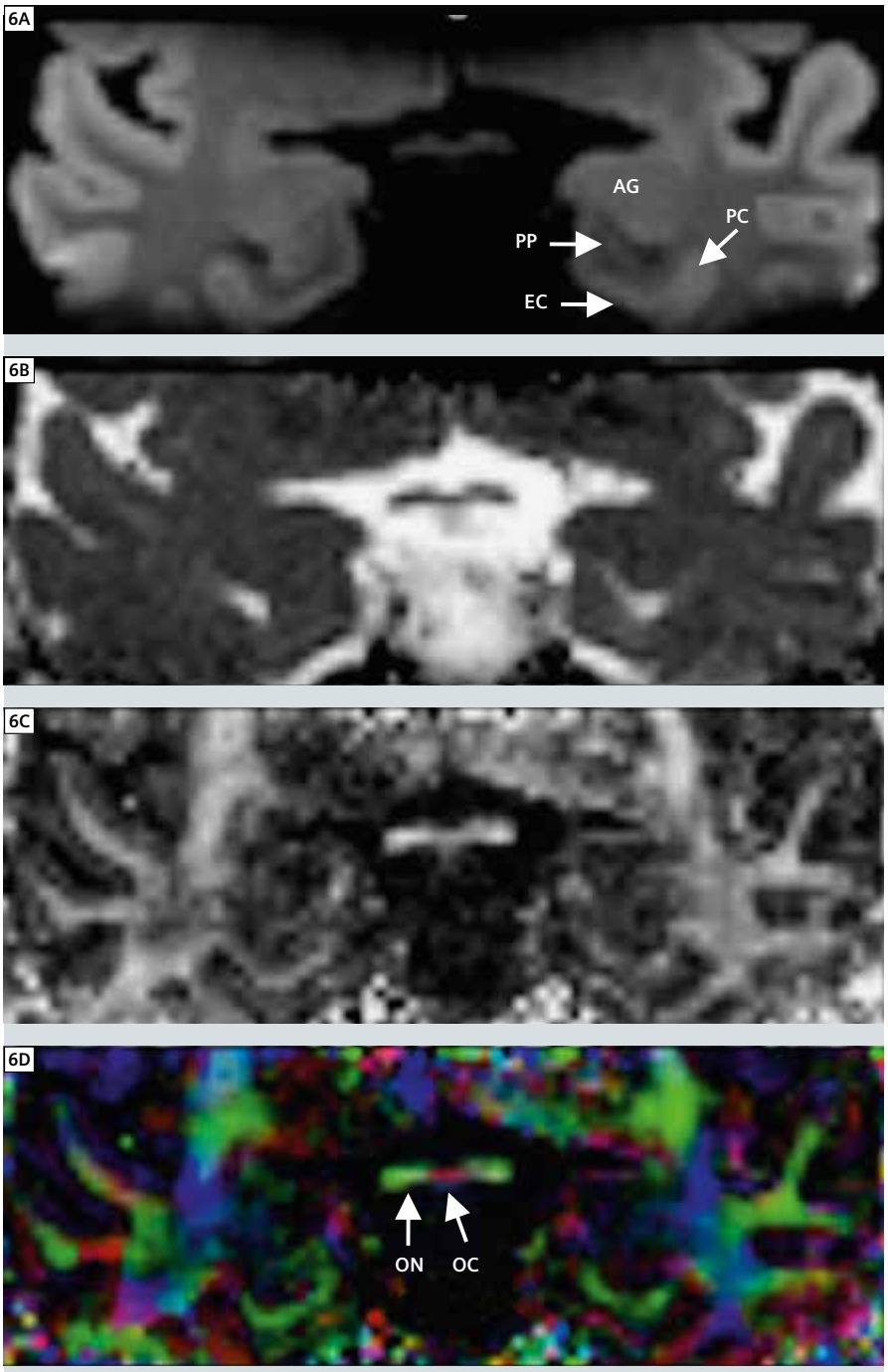

6 1.2 mm in-plane resolution reduced FOV diffusion tensor images of the medial temporal lobes using the *syngo* ZOOMit application with single-shot EPI (top to bottom: diffusion trace, ADC, FA and color orientation map). This particular coronal slice at the level of the uncus and amygdala (AG) demonstrates distortion-free quantitative diffusion in several regions affected by early Alzheimer's disease including the perirhinal cortex (PC), entorhinal cortex (EC) and perforate pathway (PP) in the subjacent white matter. Without the reduced number of phase encoding steps enabled by ZOOMit, these structures are often severely distorted by susceptibility generated from air spaces in the subjacent temporal bone.

1.8 mm^2 vs 1.3 x 1.3 mm^2 for zoomed EPI where the FOV could be reduced from 332 to 260 mm as well as the matrix slightly increased (192 x 78 to 200 x 78). Both protocols were set up for comparable acquisition times, 3:53 min ('standard') and 3:39 min (ZOOMit). Figure 4 shows an overlay of a T1-weighted VIBE with a diffusion-weighted (*b*400) dataset in multi-planar reconstruction to illustrate the excellent co-registration and resolution. In Figure 5 the comparison between standard DW-EPI (top) with the described ZOOMit DWI protocol (bottom) is shown. There is a clear improvement regarding resolution and distortion, in this example the reduced SNR however is obvious as well. This is due to two reasons, first due to increased echo time with a longer RF pulse; but secondly also a *higher resolution* protocol was acquired. In signal-starved situations, such as fatty breasts higher averaging might still be advised. Clinically, the higher spatial resolution allows the more accurate DWI evaluation of enhancing foci and small non-mass enhancement on MRI. ZOOMit DWI shows potential to mitigate spatial distortions commonly observed in standard EPI. Further developments and investigations are anticipated to balance SNR and spatial resolution, as well as a quantitative comparison including measured ADC and reduction of artifacts. The preliminary data suggest that using ZOOMit DWI can enable higher spatial resolution in breast applications at reduced distortions when supported by sufficient SNR.

Medial Temporal lobe imaging

The hippocampus and entorhinal cortex form a critical neuronal circuit for declarative memory formation that is often altered by different pathologies, including Alzheimer's disease. Unfortunately, standard single-shot EPI DTI fails to properly characterize the medial temporal lobe structures and their functional connectivity due to geometric distortions from subjacent temporal bone airspaces. In this setting, the 2D-selective RF exci-

tation approach using a Skyra pTX system can be used to overcome these distortions at 3T and, therefore, quantify diffusion tensor properties for specific medial temporal lobe structures.
To evaluate the role of ZOOMit EPI in this setting, five healthy human volunteers were imaged using the 20-channel head/neck receive coil. Single-shot EPI diffusion-weighted images with fat saturation were obtained (TR 2200 ms, TE 83 ms, NEX 15, acquisition time 8 min, 10 gradient directions, *b*800 s/mm^2) using ZOOMit EPI. The protocol used a 13.3 x 4.4 cm FOV (read x-phase axes) with 1.5 mm in-plane resolution (90 x 30 image matrix). 18 contiguous 3 mm thick oblique coronal slices were obtained orthogonal to the long axis of the temporal lobe with the most posterior slice prescribed tangential to the vertical portion of the hippocampal tail. ZOOMit DW images had acceptable signal-to-noise (6.6 ± 1.1 @ *b*800 s/mm^2) and significantly reduced geometric distortions from subjacent temporal bone airspaces compared to full FOV acquisitions. Diffusion-weighted images resolved specific components of the medial temporal lobes such as the entorhinal cortex (EC), perforant pathway white matter (PP), hippocampal head, subiculum, dentate gyrus (DG), molecular and neuronal layers of the hippocampus (CA1). Quantitative data (Table 2) was consistent with prior DTI parameter values from human hippocampus autopsy samples [5]. Color fiber orientation maps demonstrated coherence from CA1 neuron apical dendrites as previously shown [5] and data may allow tractography of the perforant pathway between the entorhinal cortex and hippocampus. The central portion of the color fiber orientation map (Fig. 6) also demonstrates the midline optic chiasm (OC, red) and paired, anterior coursing optic nerves (ON, green, 4.5 mm diameter). This is a nice illustration of the capability for ZOOMit diffusion to also achieve sufficient resolution to accurately measure diffusion parameters in cranial nerves. Similar results have been observed for the trigeminal nerves and may provide improved diagnosis/monitoring for trigeminal neuralgia.

Table 2: Quantitative diffusion values using zoomed diffusion.

Region	Mean diffusivity (x 10-3 mm^2/s)	Fractional Anisotropy
CA1	0.82 ± 0.04	0.25 ± 0.06
DG	0.86 ± 0.06	0.27 ± 0.06
ERC	0.77 ± 0.08	0.32 ± 0.07
PP	0.81 ± 0.07	0.40 ± 0.08

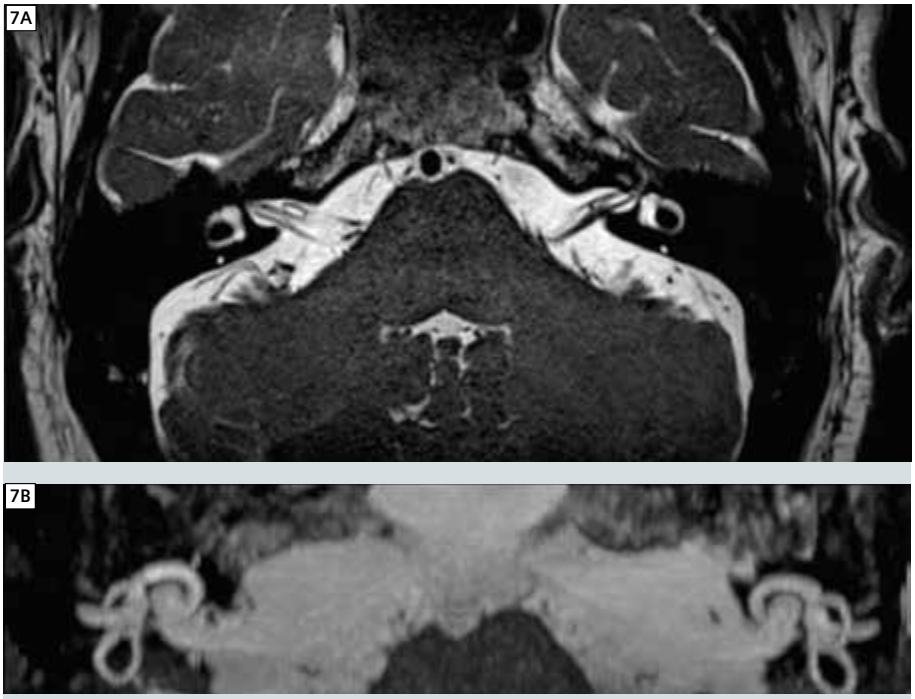

7 Zoomed T2-weighted SPACE of the IAC **(7A)** and thin maximum intensity projection **(7B)**.

ZOOMit SPACE

Similarly to ZOOMit EPI, SPACE with reduced FOV using ZOOMit can increase acquisition efficiency enabling improved spatial resolution or T2-weighting for a given scan duration. For example, ZOOMit SPACE was acquired using the 20-channel head/neck receive coil to visualize the internal auditory canal (IAC) in a patient with Meniere's disease (axial orientation, TR 1000 ms, TE 125 ms, 2 averages, echo train length of 54, 160 x 80mm FOV, 2 x 2 x 0.5 mm resolution, flip angle 100 degrees, BW: 255 Hz/Px, acquisition time 2:31 min). The acquisition time in this case was approx. 50% shorter then with the non-zoomed reference protocol. As shown in Figure 7, this

case shows clear anatomical features including cochlear and vestibular nerves, as well as posterior and lateral semi-circular canals in an axial slice (top) and thin maximum intensity projection (bottom). Another application is depicted in Figure 8 using ZOOMit SPACE in the prostate. This example was acquired using a combination of the body-18 and spine coil elements. TR 2000 ms, TE 99 ms, echo train length of 57 and 600 Hz/pixel at 320 x 160 matrix and 72 slices; using a 230 x 115 FOV this resulted in a voxel size of 0.7 x 0.8 x 1 mm at a total acquisition time of 7:15 min providing the capabilities of reformatting the data in any orientation.

Conclusions

The results shown clearly demonstrate that 2D-selective RF excitation on a 2-channel pTX system enables zoomed EPI acquisitions on 3T scanners that can significantly reduce the limitations imposed by spatial distortions due to field inhomogeneity. Together with the inherent ability to simultaneously improve excitation inhomogeneity while providing effective reduced FOV implementations, the TimTX TrueShape clinical platform is ideally suited to fully capitalize on a wide range of improved imaging approaches that require a practical and fully integrated multi-channel transmission platform. These approaches have been previously demonstrated to be of significant value in similarly challenging imaging settings, albeit at the expense of requiring a complex hardware set up due to the lack of commercially available, fully-integrated, multi-channel transmission platforms. The introduction of the clinical Skyra TimTX TrueShape platform is poised to have a significant impact on the clinical implementation of such powerful imaging tools.
For further scientific details of the above shown studies, please refer to Proc ISMRM 2013 abstract numbers (#): #3390 (prostate), #1554 (kidney), #1739 (breast), #3021 (neuro).

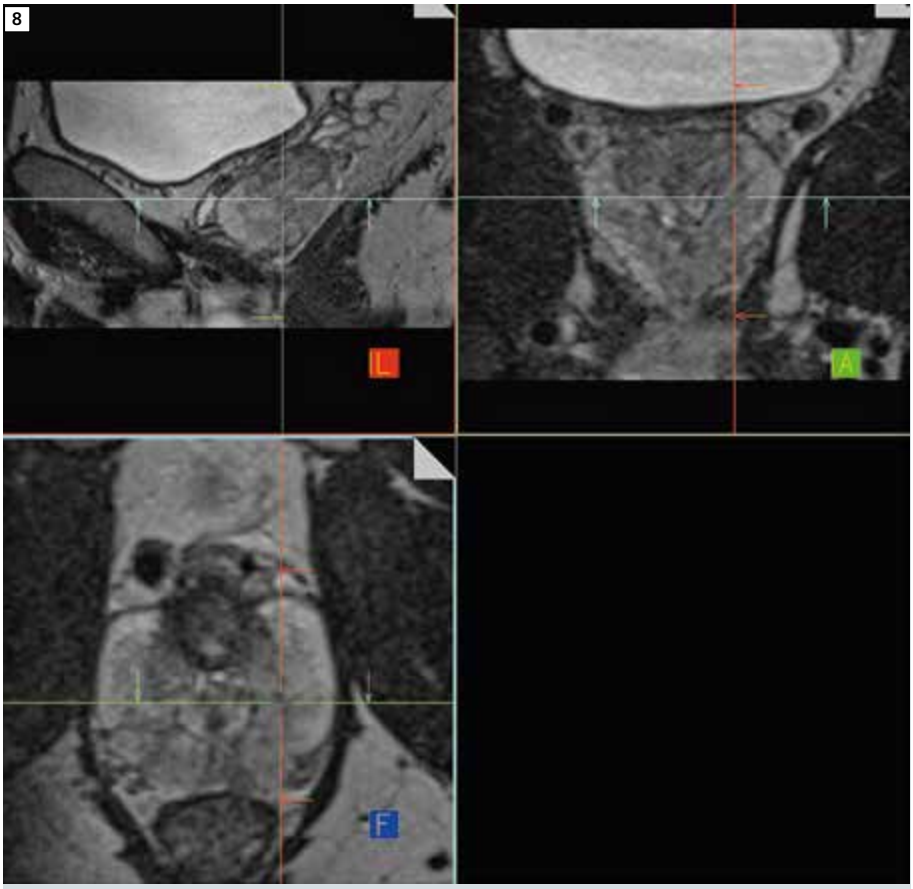

8 Zoomed T2-weighted SPACE of the prostate (MPR).

References

1 Rieseberg S, Frahm J, Finsterbusch J. Two-dimensional spatially-selective RF excitation pulses in echo-planar imaging. Magn Reson Med. 2002 Jun;47(6):1186-93.
2 Schneider R et al. Evaluation of 2D RF echo planar pulse designs for parallel transmission. Proc ISMRM 2012 #3459.
3 Ries M, et al. Diffusion tensor MRI of the human kidney. JMRI 2001;14(1):42-49.
4 Notohamiprodjo M et al. Diffusion tensor imaging of the kidney with parallel imaging: Initial clinical experience. Invest Radiol 2008;43(10):677-685.
5 Sigmund EE et al. Intravoxel incoherent motion and diffusion-tensor imaging in renal tissue under hydration and furosemide flow challenges. Radiology 2012;263(3):758-769.
6 Shepherd TM et al. diffusion tensor microscopy indicates the cytoarchitectural basis for diffusion Anisotropy in the human hippocampus. AJNR 2007;28:958-964.

Contact
Fernando Boada
Department of Radiology
NYU Langone Medical Center
660 1st Avenue
New York, NY 10016
USA
fernando.boada@nyumc.org

Notes

On account of certain regional limitations of sales rights and service availability, we cannot guarantee that all products included in this brochure are available through the Siemens sales organization worldwide. Availability and packaging may vary by country and is subject to change without prior notice. Some/All of the features and products described herein may not be available in the United States.

The information in this document contains general technical descriptions of specifications and options as well as standard and optional features which do not always have to be present in individual cases.

Siemens reserves the right to modify the design, packaging, specifications and options described herein without prior notice. Please contact your local Siemens sales representative for the most current information.

Note: Any technical data contained in this document may vary within defined tolerances. Original images always lose a certain amount of detail when reproduced.

Order No. A911IM-MR-14442-P1-4A00
Printed in USA 01-2014 | All rights reserved
© 2014 Siemens Medical Solutions USA, Inc.

Local Contact Information
Siemens Medical Solutions USA, Inc.
51 Valley Stream Parkway
Malvern, PA 19355-1406
USA
Telephone: +1-888-826-9702
www.usa.siemens.com/healthcare

Global Business Unit
Siemens AG
Medical Solutions
Magnetic Resonance
Henkestr. 127
DE-91052 Erlangen
Germany
Telephone: +49 9131 84-0
www.siemens.com/healthcare

Global Siemens Headquarters
Siemens AG
Wittelsbacherplatz 2
80333 Muenchen
Germany

Global Siemens Healthcare Headquarters
Siemens AG
Healthcare Sector
Henkestrasse 127
91052 Erlangen
Germany
Telephone: +49 9131 84-0
www.siemens.com/healthcare

Legal Manufacturer
Siemens AG
Wittelsbacherplatz 2
DE-80333 Muenchen
Germany

www.siemens.com/healthcare